ZANCO Journal of Pure and Applied Sciences
The official scientific journal of Salahaddin University-Erbil
https://zancojournals.su.edu.krd/index.php/JPAS

ISSN (print):2218-0230**, ISSN (online):** 2412-3986**, DOI: http://dx.doi.org/10.21271/zjpas**

RESEARCH PAPER

Optimization of Variable Parameters in Diode Pumped SHG Nd-YAG Lasers

Twana Mohammed Kak Anwer [1*], Nahlah Mohammed Qadir [2], and Suran Dunun Yaseen[3]
[1, 2] Department of Physics, College of Education, Salahaddin University-Erbil, Kurdistan Region, Iraq
[3] Department of Information Technology, Khabat Technical Institute, Erbil Polytechnic University, 44001 Erbil, Iraq

A B S T R A C T:
Second Harmonic Generation (SHG) is the process of doubling the natural frequency of any laser. Since the output of Nd-YAG lasers has a wavelength of $1.064\mu m$, it is the aim of this research to produce an SHM diode pumped of this laser with a wavelength of $0.532\mu m$. This work is done via manipulating a few equations to produce the best results for both circulating and keeping other input parameters constant such as reflectivity, and amplification factor, on other cavity engineering parameters. The results are compared with other experimental values, and they are in fair agreement within the chosen incident powers, ranging from one to sixteen milliwatts. Also, a tendency is performed to perform a modification for the reflectivity of the crystal end reflectivity, which is the theory-built proposal. But the fact is that for the [MgO: LiNbO3] crystal only (0.992) the reflectivity enhances the other parameters such as the round-trip transmission, the second harmonic time duration, and the second harmonic efficiency of the crystal.

KEY WORDS: Nd-YAG Laser, SHG using MgO: LiNbO3, Powers.
DOI: http://dx.doi.org/10.21271/ZJPAS.35.2.5
ZJPAS (2023) , 35(2);41-47 .

1.INTRODUCTION :

Generally, Second Harmonic Generation occurs in crystals which have non-linear optical properties. The circulating power P_c is generated almost in the external or second cavity whose optical properties are not monolithic, since few are affected by thermal and mechanical sources within the system (Xiong et al., 2021, de Lima et al., 2022). In this study a diode-pumped Nd-YAG, with a fundamental wavelength of $1.064\mu m$ is converted to a frequency doubled beam of $0.532\mu m$ via second harmonic generation. The second harmonic efficiency of these lasers is high compared to those of gas and CW diode lasers. The parameters needed for controlling the operation are both the cavity reflectance parameter R_m and the circulating power P_c, inside the harmonic resonator. Theoretically P_c depends on R_m in a way that they are called the constants of the resonator.

* **Corresponding Author:**
Twana Mohammed Kak Anwer
E-mail: twana.anwar1@su.edu.krd
Article History:
Received: 06/07/2022
Accepted: 08/10/2022
Published: 20/04 /2023

In each of them, a monolithic crystal has been employed in the external cavity, the mostly known are KDP (Potassium Dihydrogen Phosphate) and ADP (Ammonium dihydrogen phosphate) crystals which are of use to calculate their physical properties (Chen et al., 2012).
In 1966, Ashkin, (Ashkin et al., 1966, Mehta and Rampal, 1993) tried the circumstance of the second cavity to enhance the fields present in it. After that, in 1981, Breiger, (Brieger et al., 1981) developed the necessities of the external cavity as increasing the reflectance of the first external cavity M_1 to 95%. Finally, in 1987, Kozlovsky (Kozlovsky et al., 1988) tried to overcome the poor efficiency of the SHG cavity by increasing the reflectance of the first mirror in the external cavity to 97%. The process was via neglecting the absorbance of the second mirror M_2 of the second cavity, representing the reflected power on the surfaces of the crystal to be unity. This produced about 13% of the output an efficiency of the SH external power (Mari et al., 2021).

It is the aim of this study to calculate theoretically the optimum values for both the circulating power P_c and the reflecting power P_r within the ranges of their corresponding experimental powers performed by Kozlovsky and others (Kozlovsky et al., 1988) (Mari et al., 2021).
In fact, the realities tell that the imperfectness of the crystal ends pushes the output power to circulate P_c around the crystal, creating another portion of the fundamental power to what is called the reflecting power P_r. The mirrors, reflecting at the fundamental and transmitting at the second harmonic, are applied directly to the polished crystal ends as shown in figure (**1**).

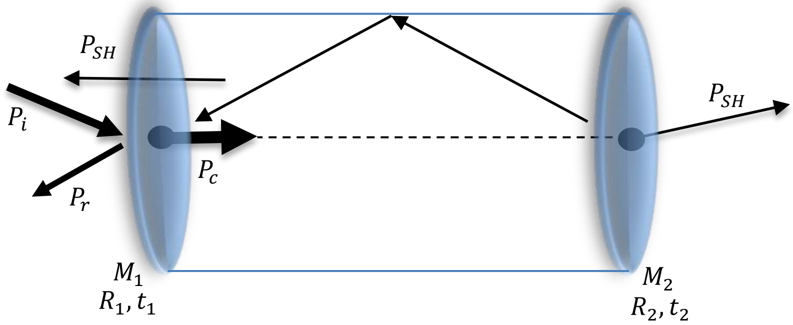

Figure (1): Standing wave geometry for monolithic crystal resonators.

In this way, the two new coefficients are R_m and R_1 which are both high for typical cavities.

2. Methodology

The background theory of the process, and the outline of the results are manipulated and the equation necessary for our calculations are processed.
Once the first harmonic efficiency γ_{SH} is defined, the effort of Ashkin, Boyd, and Dziedzic (Ashkin et al., 1966, Altiere, 2014) known as ABD formulae is produced.
They defined the second harmonic transmittance t_{SH} firstly as the power factor P_c, circulating power multiplied by SH coefficient γ_{SH}:

$$t_{SH} = 1 - \gamma_{SH}\, P_c \;..(1)$$

The conversion efficiency of the resonated fundamental to the second harmonic is given by:

$$\eta_{SH} = \gamma_{SH}\, P_c \;..(2)$$

For most monolithic crystals with proper effective non-linear conversion factor ($d = 5.95 \times 10^{-12}\,\frac{m}{V}$) for MgO: $LiNbO_3$ crystal, then (Byer, 1975, Guo and Wang, 2017, Chaitanya et al., 2016):

$$\gamma_{SH} = \left(\frac{2\, f^2\, d^2}{\pi\, \lambda\, n^3\, \varepsilon_0\, c^3}\right) Lh(\beta, \alpha) \;..(3)$$

where $h(\beta,\alpha), f, \lambda, n, c$, and ε_0 are the Boyd and Kleinman focusing factors, with the double refraction parameter β and focusing parameter α, the laser fundamental frequency, the fundamental wavelength of the laser ($\lambda = 1064nm$), the refraction index of the crystal, the light speed, and the permittivity of free space ($\varepsilon_0 = 8.8542 \times 10^{-12}\,\frac{\sec^4 A^2}{m^3\,Kg}$), respectively.
Here the complex parameter $Lh(\beta,\alpha)$ is the function of the crystal length and the vertical component of the double refraction parameter β.

The unique parameters (physical and geometrical) properties of the MgO: $LiNbO_3$ crystal is tabulated below.

Table (1): Parameters of monolithic external cavity frequency doubling crystals (Kozlovsky et al., 1988, Wang et al., 2016).

Parameter name	Parameter	Value
single harmonic efficiency	γ_{SH}	$0.0025\ W^{-1}$
reflectance of M_1 and M_2	$R_1 = R_2$	0.997
transmittance of M_1	$t_1 = 1 - R_1$	0.003
Roundtrip transmission	t^2	0.992

Figure (**2**) is the product of the structural shape of the figure (**1**) (Kozlovsky et al., 1988).
In figure (**2**), the solid line is the trendline polynomial processed using the MATLAB program. The dot points are experimental values used by Kozlovsky (Kozlovsky et al., 1988).

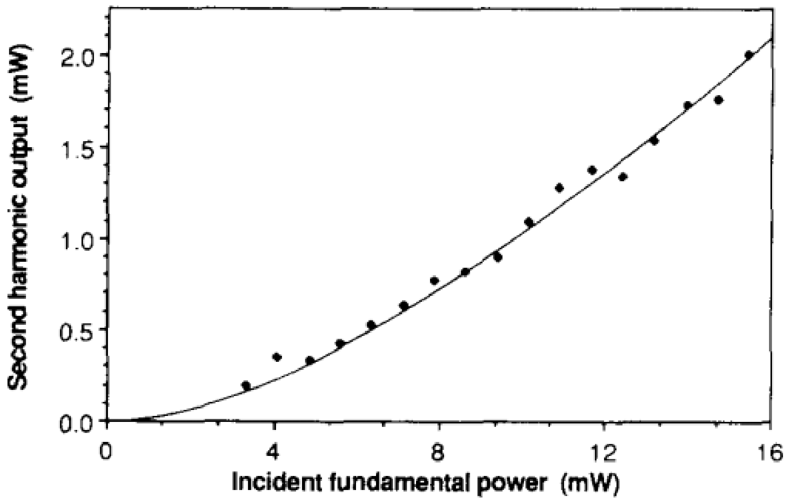

Figure (2): Represents variation of second harmonic power P_{SH} as the function of fundamental powerP_i for MgO: LiNbO3 crystal (Kozlovsky et al., 1988).

Depending on the background of the parameters used in the second cavity the value of P_r and P_c could be both found, depending on their definition giver by Kozlovsky (Kozlovsky et al., 1988, Aspelmeyer et al., 2014) as:

$$P_c = \frac{t_1}{\left(1-\sqrt{R_1 R_m}\right)^2}\, P_i \, ..(4)$$

$$P_r = \frac{\left(\sqrt{R_1}-\sqrt{R_m}\right)^2}{\left(1-\sqrt{R_1 R_m}\right)^2}\, P_i \, ..(5)$$

$$\therefore\ \frac{P_r}{P_c} = \frac{\left(1-\sqrt{R_1 R_m}\right)^2}{t_1} \, ..(6)$$

where, t_1, R_1 and R_m are transmittance of M_1, reflectance of M_1 and the cavity reflectance parameter defined by the own round transmittance of the transmittance term of equation (1) the reflectance of M_2, respectively.

The proportionality between them is the square of the complex round transmittance (t^2) to be 0.992.

The cavity reflectance parameter for the standing wave geometry, which generates green color in both directions is given by (Sergeeva et al., 2021, Villarreal and Armenta, 2021):

$$R_m = t^2 t_{SH}^2\, R_2 \, ..(7)$$

The second harmonic efficiency is the ratio between the SH power to the circulating power as (Fürst et al., 2010):

$$\eta_{SH} = \frac{P_{SH}}{P_c} \, ..(8)$$

From this, we obtain SH power for the standing wave geometry as (Karimi et al., 2021, Ilinskii et al., 1998):

$$P_{SH} = 2\, \gamma_{SH}\, P_c^2 \, ..(9)$$

which represents the sum of the forward and backward propagating second harmonic outputs.

3. Results and Discussion

Our calculations were direct applications of equations (4) and (5) within the allowed range of fundamental or incident power from one to sixteen. The values of R_m were calculated using equation (1), keeping the values of t^2 and R_1 constant, and t_{SH} was a variable calculated from equation (1). Here, most calculations have been performed neglecting thermal and mechanical effects, which were taken into consideration practically **(**Wang et al., 2016**)**. Mechanical effects include vibrations and end detachments of the crystal, plus the possibility of screws and touching fairly.

The aim was to get all previous experimental tendencies in the past five decades [1965-2015], where the theory was completed for this non-linear crystal. Finally, all functions of the fundamental power P_i and the second cavity reflectance and transmittance parameters (R_1, t_1, and R_m) which are all defined well in the theory defined.

These are shown in figures (**3**, **4**, **5**, and **6**) schematically. All of these power types (P_i, P_{SH}, P_c, and P_r) have their own importance and benefit in the improving the SH efficiency of the second cavity power.

The value of P_i, P_{SH}, P_c, R_m, and P_r are shown in table (**2**). Where the data of both P_i and P_{SH} are obtained from Kozlovsky results which is shown in figure (**2**).

The values of P_c for a standing wave geometry found using equation (9) for each value of P_{SH} considering is $\gamma_{SH} = 0.0025\ W^{-1}$.

Also, the value of R_m is obtained using equation (4) where both R_1 and t_1 are determined in table (**1**) for each value of P_i and P_c. After that, the optimum value of R_m is found in figures (**4**, **5**, and **6**) using the value of their slopes.

Also, the value of P_r is determined using equation (5) for each value of P_i and R_m, remembering that equation (5) was the value of $R_1 = 0.997$, as shown in table (**1**).

Table (2): Parameter of powers for MgO: LiNbO$_3$ crystal.

$P_i\ (mW)$	$P_{SH}\ (mW)$	$P_c\ (mW)$	R_m	$P_r\ (mW)$
3.3380	0.1889	6.1467	0.9237	2.8688
4.0778	0.3498	8.3642	0.9278	3.4735
4.8949	0.3254	8.0670	0.9192	4.2434
5.5985	0.4188	9.1520	0.9189	4.8564
6.3764	0.5292	10.2878	0.9184	5.5367
7.1172	0.6311	11.2347	0.9175	6.1899
7.8574	0.7667	12.3831	0.9174	6.8345
8.5990	0.8180	12.7910	0.9149	7.5111
9.4143	0.9032	13.4401	0.9132	8.2472
10.1166	1.0893	14.7601	0.9141	8.8488
10.8560	1.2755	15.9717	0.9145	9.4899
11.6710	1.3775	16.5980	0.9130	10.2268
12.3769	1.3445	16.3982	0.9098	10.8982
13.1533	1.5391	17.5450	0.9101	11.5765
13.9296	1.7338	18.6214	0.9102	12.2580
14.7088	1.7599	18.7610	0.9081	12.9843
15.4101	2.0050	20.0250	0.9089	13.5866
Average R_m:			0.9152	

Figure (**3**) shows the variation of both P_{SH} and P_c theoretically, where they are almost coincident to each other. Also, from figure (**3**) the value of SH coefficient for a standing wave cavity geometry using equation (9) was $\gamma_{SH} = 0.0025\ W^{-1}$, and this is the same value found by Kozlovsky practically using equation (3) for [MgO: LiNbO$_3$] crystal.

Figure (**4**) shows the dependence of circulating power P_c on the fundamental power P_i both theoretical and experimental results are considered keeping in mind the optimum value for R_m was necessary to be calculated.

Figure (**5**) represents the variation P_r as the function of P_i in mW units, but the perfectness of the first mirror was considered (i.e.: $R^2 = 1$). From the experimental values and according to the ideal condition of the value of R^2 our data was completely agreed with theoretical value. Because the ideal crystal is assumed to be a perfect reflector (Mari et al., 2021).

It is noticed that for each of figures (**4**) and (**5**) and from their slopes, the value of R_m (as optimum) is the same which is 0.9122.

Finally, for comparison, the values of P_r against P_c are plotted in figure (**6**) taking the maximum calculated value of R^2 experimentally. It is noticed that in figure (**6**) and from its slope, the value of R_m (as optimum) is 0.9182.

Generally, the results show the following notifications:

1. The optimum value of the second harmonic coefficient γ_{SH} is calculated using equation (3) and the parameters shown in table (**1**).
2. When the second harmonic power is calculated, the circulating power was observed also that it is the indirect function of P_i. This means that P_c is constant for a complete round trip with P_i, but it changes with the fluctuations of thermal and mechanical circumstances of the external cavity.
3. Ideally, if the reflected power P_r is considered to be zero, as theory indicates for that Kozlovsky (Kozlovsky et al., 1988, Scruby and Drain, 2019), it was clear that it is slightly changed as t^2 is 0.992, but experimentally, this result changes according to the imperfectness of the crystal ends and also due to thermal effects inside the cavity. This means that the maximum reflectance of the second mirror M_2 of the external cavity has the value of (0.008) as it is observed in figure (**4**).

Finally, the value of cavity reflectance parameter R_m is the function of two constants of the external cavity (t^2 and R_2) and one secondary variable, the second harmonic transmittance t_{SH}. This conclusion pushes as t_{SH} as in equation (1) keeping $\gamma_{SH} = 0.0025\ W^{-1}$.

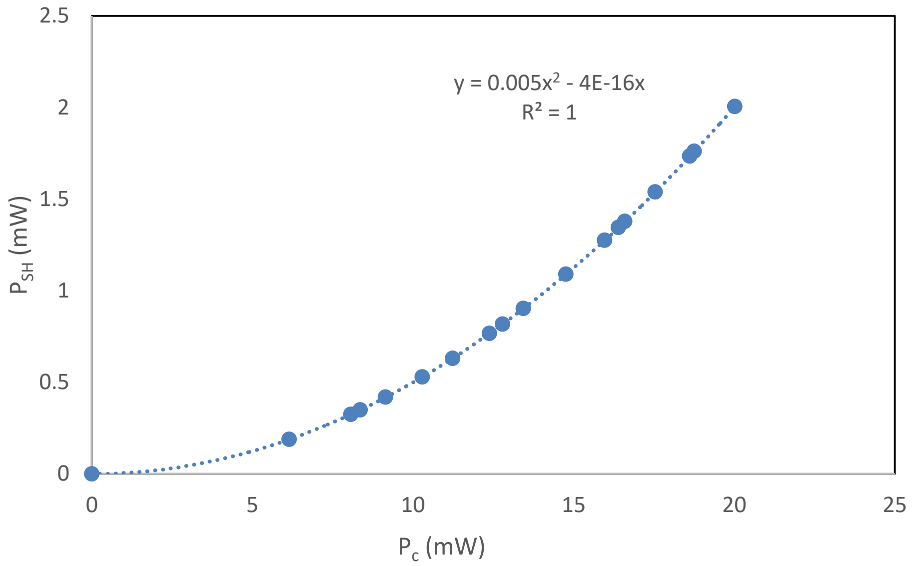

Figure (3): Represents variation of second harmonic power P_{SH} as the function of circulating power P_c for MgO: $LiNbO_3$ crystal.

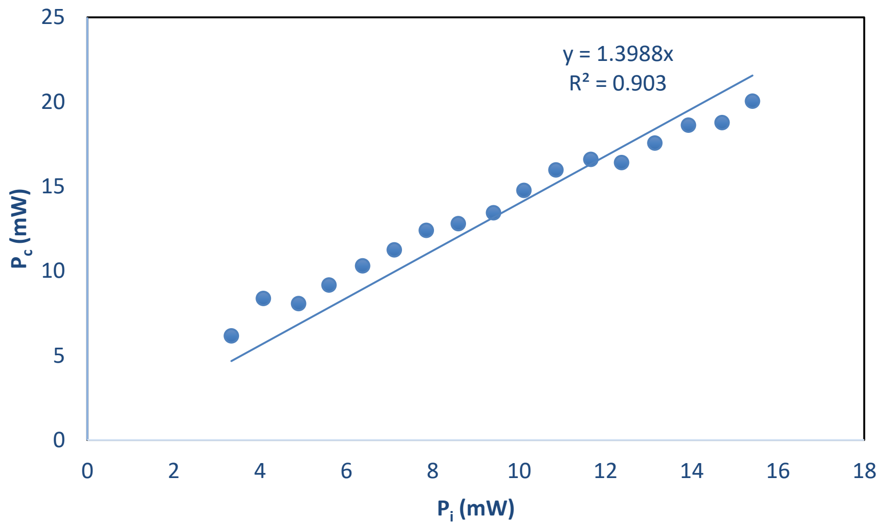

Figure (4): Represents variation of circulating power P_c as the function of fundamental power P_i for MgO: $LiNbO_3$ crystal.

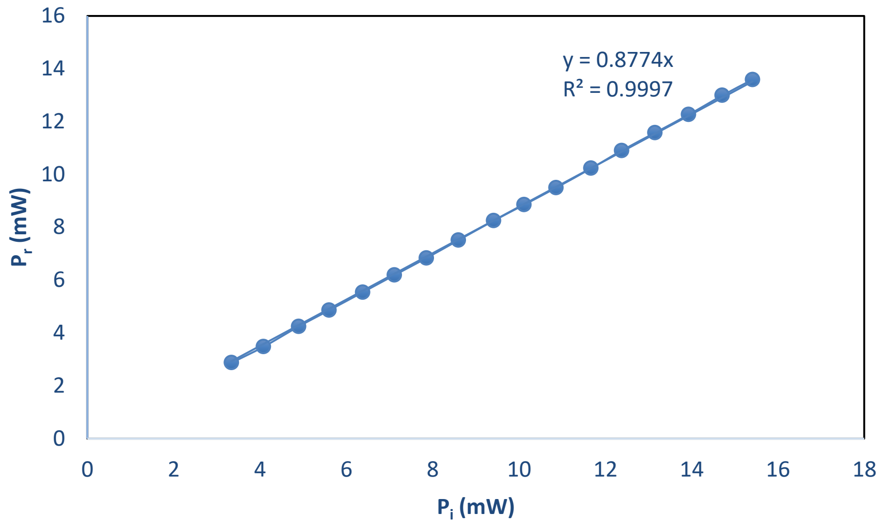

Figure (5): Represents variation of reflecting power P_r as the function of fundamental power P_i for MgO: LiNbO$_3$ crystal.

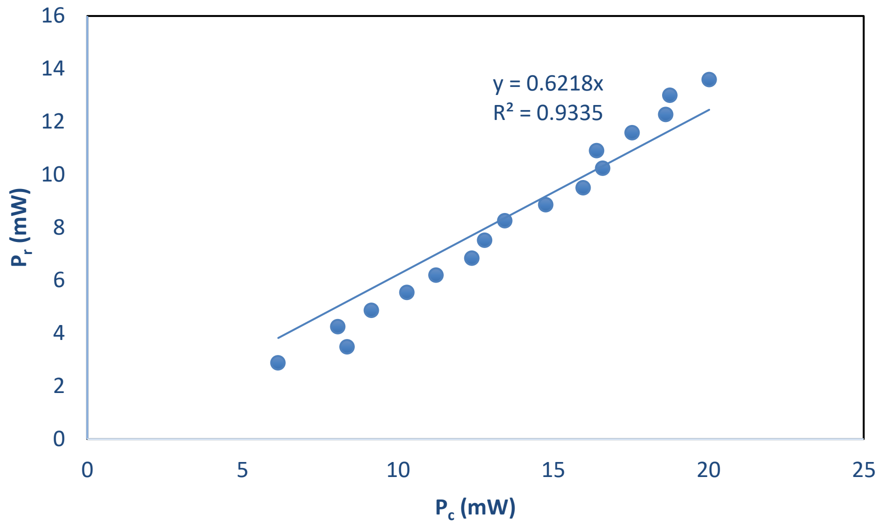

Figure (6): Represents variation of reflecting power P_r as the function of circulating power P_c for MgO: LiNbO$_3$ crystal.

4. Conclusion

The overall comprehension leads to a few important and fundamental new changes and surprises in the process of second harmonic power, since the unexpected and new existence for some parameters, leads to be said that:

1. Thermal imperfections of the external cavity and fluctuations in some optical parameters of [MgO: LiNbO$_3$] crystal, pushes the cavity reflectance parameter to change slightly while keeping the optimal values as 0.9122 and 0.9182.
2. The minimum value for R_m was 0.9081, calculated from equation (7) keeping t^2 and R_2 constants with maximizing t_{SH} from equation to be 0.9582. This is coming from the maximum capacity of the second cavity for P_c value to be round $600mW$.
3. Variation of P_r with P_c in figure (**6**) is a random process depending on the value of R^2 which was 0.9908 as optimum, but varied experimentally up to 0.997. This means that, theoretically it could be considered as constant of the cavity.
4. The results of optimum Rm are equal 0.9122 as revealed in figures (4) and (5) while it is 0.9182 in figure (6), employing their slopes and equations (4, 5, and 6). The average R_m is 0.9152 as shown in table (2). So, the difference between the optimums of R_m and average Rm is the

value of transmittance ($t_1 = 0.003$) as represented in table (1).

5. In future, many fields and applications are predicted to be performed experimentally among them:

A. Applying the category of these calculations in this study for other gas and solid-state lasers such as excimer and ruby lasers.
B. Keeping and controlling thermal and optical properties of the crystals such as KDP and ADP, to be constants, stimulating researchers to do more improvements on P_c and P_r.
C. Possibility of generating higher harmonic generations, 2^{nd} HG, for example could be processed for low power gas lasers such as He-Ne Laser.

5. References

ALTIERE, E. E. 2014. *The adventures of Nikita and Casper: high power ultraviolet lasers for precision spectroscopy.* University of British Columbia.

ASHKIN, A., BOYD, G. & DZIEDZIC, J. 1966. Resonant optical second harmonic generation and mixing. *IEEE Journal of quantum electronics,* 2**,** 109-124.

ASPELMEYER, M., KIPPENBERG, T. J. & MARQUARDT, F. 2014. Cavity optomechanics. *Reviews of Modern Physics,* 86**,** 1391.

BRIEGER, M., BÜSENER, H., HESE, A., MOERS, F. V. & RENN, A. 1981. Enhancement of single frequency SGH in a passive ring resonator. *Optics Communications,* 38**,** 423-426.

BYER, R. 1975. Parametric oscillators and nonlinear materials. *Nonlinear Optics*, 2.

CHAITANYA, N. A., AADHI, A., KUMAR, S. C., JABIR, M., SAMANTA, G. & EBRAHIM-ZADEH, M. 2016. Frequency-doubling of femtosecond pulses in "thick" nonlinear crystals with different temporal and spatial walk-off parameters. *IEEE Photonics Journal,* 8**,** 1-13.

CHEN, C., SASAKI, T., LI, R., WU, Y., LIN, Z., MORI, Y., HU, Z., WANG, J., AKA, G., YOSHIMURA, M. AND KANEDA, Y., 2012. Nonlinear optical borate crystals: Principals and applications. John Wiley & Sons.

DE LIMA, T. F., DORIS, E. A., BILODEAU, S., ZHANG, W., JHA, A., PENG, H.-T., BLOW, E. C., HUANG, C., TAIT, A. N. & SHASTRI, B. J. 2022. Design Automation of Photonic Resonator Weights. *arXiv preprint arXiv:2203.01792*.

FÜRST, J., STREKALOV, D., ELSER, D., LASSEN, M., ANDERSEN, U. L., MARQUARDT, C. & LEUCHS, G. 2010. Naturally phase-matched second-harmonic generation in a whispering-gallery-mode resonator. *Physical review letters,* 104**,** 153901.

GUO, S. & WANG, J. 2017. Efficient generation of a continuous-wave, tunable 780 nm laser via an optimized cavity-enhanced frequency doubling of 1.56 µm at low pump powers. *Optical and Quantum Electronics,* 49**,** 1-16.

ILINSKII, Y. A., LIPKENS, B., LUCAS, T. S., VAN DOREN, T. W. & ZABOLOTSKAYA, E. A. 1998. Nonlinear standing waves in an acoustical resonator. *The Journal of the Acoustical Society of America,* 104**,** 2664-2674.

KARIMI, F., SOLEIMANIKAHNOJ, S. & KNEZEVIC, I. 2021. Tunable plasmon-enhanced second-order optical nonlinearity in transition metal dichalcogenide nanotriangles. *Physical Review B,* 103**,** L161401.

KOZLOVSKY, W. J., NABORS, C. & BYER, R. L. 1988. Efficient second harmonic generation of a diode-laser-pumped CW Nd: YAG laser using monolithic MgO: LiNbO/sub 3/external resonant cavities. *IEEE journal of quantum electronics,* 24**,** 913-919.

MARI, M. A., MEMON, Z. A., SHAIKH, P. H., MIRJAT, N. H. & SOOMRO, M. I. 2021. A review study on mathematical modeling of solar parabolic d ish-Stirling system used for electricity generation. *International Journal of Energy Research,* 45**,** 18355-18391.

MEHTA, P. C. & RAMPAL, V. 1993. *Lasers and holography*, World Scientific.

SCRUBY, C. B. & DRAIN, L. E. 2019. *Laser ultrasonics: techniques and applications*, Routledge.

SERGEEVA, K. A., SERGEEV, A. A., MININ, O. V. & MININ, I. V. A Closer Look at Photonic Nanojets in Reflection Mode: Control of Standing Wave Modulation. Photonics, 2021. Multidisciplinary Digital Publishing Institute, 54.

VILLARREAL, J. M. G. & ARMENTA, J. A. G. 2021. Quantification of the field enhancement of surface plasmon under standing wave conditions. *Plasmonics***,** 1-10.

WANG, J., ZHANG, K., GE, Y. & GUO, S. 2016. Efficient frequency doubler of 1560 nm laser based on a semi-monolithic resonant cavity with a PPKTP crystal. *Optics Communications,* 369**,** 194-198.

XIONG, M., LIU, M., JIANG, Q., ZHOU, J., LIU, Q. & DENG, H. 2021. Retro-reflective beam communications with spatially separated laser resonator. *IEEE Transactions on Wireless Communications,* 20**,** 4917-4928.

Conflict of Interest

The authors confirm that there is no conflict of interest.